International Journal of GEOMATE, Aug. 2023, Vol. 25, Issue 108, pp.122-129
ISSN: 2186-2982 (P), 2186-2990 (O), Japan, DOI: https://doi.org/10.21660/2023.108.3534
Geotechnique, Construction Materials and Environment

THREE-DIMENSIONAL PHYSICAL MODELLING OF SINGLE CHAMBER SKIRT BREAKWATER (SCSB)

Azis Ali Wibowo[1], Ricky Lukman Tawekal[1], *Harman Ajiwibowo[1], and Andojo Wurjanto[1]

[1]Faculty of Civil and Environmental Engineering, Institut Teknologi Bandung, Indonesia

*Corresponding Author, Received: 28 July 2022, Revised: 1 March 2023, Accepted: 4 May 2023

ABSTRACT: The single chamber skirt breakwater (SCSB) is a skirt-type breakwater consisting of piles at the lower part and a chamber skirt without porosity in the upper part of the structure. Three-dimensional physical modeling is conducted in the wave basin to measure the effectiveness of the skirt-type breakwater by examining the transmission coefficient (C_T) and the reflection coefficient (C_R). In addition, the relationship between environment (kh, H_I/L) and structure (s/h) independent variables with the transmission and reflection coefficient are investigated. The physical modeling concluded that the structure's transmission coefficient in the intermediate-depth water region (kh between 0.32–1.11) is 0.37–0.62 and the reflection coefficient is 0.33–0.49. On the other hand, in the shallow water region, kh is in the range of 0.21–0.30, the transmission coefficient is 0.50–0.56, and the reflection coefficient is in the range of 0.36–0.48. Therefore, it is concluded that the SCSB is effective in intermediate-depth water and not in shallow-water regions.

Keywords: Single chamber skirt breakwater, Transmission coefficient, Reflection coefficient, Intermediate depth water, Three-dimensional physical modeling.

1. INTRODUCTION

The construction of a skirt-type pile breakwater, such as the SCSB, in intermediate and deep water regions is more efficient than constructing a rubble mound breakwater. The SCSB type is more economical in terms of the quantity of material, less maintenance, and a smaller environmental impact during construction [1]. The research investigated the effectiveness of the SCSB using three-dimensional (3D) physical modeling in a wave basin. The physical modeling is carried out in the Ocean Engineering Laboratory at Bandung Institute of Technology, Indonesia.

Previous research conducted by Suh et al. [2] observed a curtain-wall–pile breakwater using physical and analytical models in intermediate-depth to deep water. The model consisted of a vertical wall in the upper part and was supported by piles in the lower part. The research concluded that the curtain-wall–pile breakwater resulted in larger transmitted and smaller reflected waves than the pile-supported vertical wall breakwater.

A slotted breakwater, which consists of a vertical slot in one row using regular waves, was investigated by Koraim [3]. The hydrodynamic characteristics of the slotted breakwater were observed using an analytical and experimental model. The wave reflection and transmission, energy loss, and hydrodynamic forces for the various values of waves and structural parameters were investigated. The experiment concluded that the wave energy reduction was 20–50% from the incoming wave energy.

Laju et al. [4] studied the energy dissipation of a single chamber skirt-type breakwater using the Eigen function expansion of the velocity potentials in the intermediate-depth water region ($1.0 < kh < 2.6$). The study concluded that the maximum energy dissipation rate of up to 50% was produced when the chamber width was between 0.3 and $0.5L$ (L is the wavelength).

The curtain-wall–pile breakwater, modified with a circular pile, was investigated by Suh et al. [5] using mathematical modeling and validated with physical modeling. The research concluded that the transmission coefficient decreases and the reflection coefficient increases as the gaps in the pile decrease.

The effect of the two-chamber perforated breakwater in shallow water conditions was investigated by Wurjanto et al. [6]. The researchers studied the effect of the number of chambers in the breakwater in terms of the transmission coefficient. The study concluded that a breakwater with more chambers is more effective than a breakwater with fewer chambers.

Ajiwibowo [7] conducted 3D physical models of a Perforated Skirt Breakwater (PSB) to examine the structure's effectiveness through the value of the transmission coefficient (C_T). The research concluded that the PSB is adequate for shorter wave periods/higher wave steepness but not adequate for longer wave periods. For shorter waves, it can dampen the waves by up to 50%.

Ajiwibowo [8] investigated the effectiveness of a Single Curtain Pile Foundation Breakwater (SCPFB) by calculating the transmission coefficient

(C_T) in intermediate-depth water. The research concluded that the SCPFB was almost 90% effective when applied with the curtain extended to half the water depth and suggested continuing the research in the $kh>\pi$.

Ajiwibowo [9] conducted 2D physical modeling of a Perforated Skirt Breakwater (PSB) to measure the effectiveness of the structure. The investigation concluded that the PSB effectively dampens the wave energy by 30–70% for short waves (according to the C_T value).

2. RESEARCH SIGNIFICANCE

The significance of the research is to examine the effectiveness of the SCSB, which is represented by the transmission coefficient (C_T) and the reflection coefficient (C_R) relationship with the environment and structure variables in the shallow ($0.21<kh<0.30$) and intermediate depth water region ($0.32<kh<1.11$). The research also will reveal the effect of three-dimensional and two-dimensional waves on the SCSB. Two-dimensional physical modeling (2D) has been carried out previously in a wave flume [10].

3. SCALING AND DIMENSIONAL ANALYSIS

3.1 Scaling

The scaling was formulated using the Froude similarity principle as written in Eqs. (1) and (2).

$$(F_r)\text{ prototype} = (F_r)\text{ model} \tag{1}$$

$$F_r = \frac{v}{\sqrt{gL}} \tag{2}$$

F_r = Froude Number
v = flow velocity
g = gravitational acceleration
L = length dimension

From the examination of the wave basin capacity, a scale of 1:12 is used. Tables 1 and 2 show the structure and environment variables of the modeling, respectively.

3.2 Dimensional Analysis

The dimensional analysis is calculated to produce the dimensionless parameters that will vary during the modeling. The dimensional analysis uses the Buckingham Pi ($\prod$) method [11]. The dimensionless variables are stated in Eqs. (3) and (4).

$$C_T = \prod\left(kh, \frac{H_I}{L}, \frac{s}{h}, \frac{L_c}{h}\right) \tag{3}$$

$$C_R = \prod\left(kh, \frac{H_I}{L}, \frac{s}{h}, \frac{L_c}{h}\right) \tag{4}$$

C_T = transmission coefficient
C_R = reflection coefficient
$k = 2\pi/L$ = wave number
L = wavelength
L_c = length of the chamber
s = draft of the skirt
h = water depth
H_I = incident wave height

The dimensionless variables to be examined are the correlation between the transmission (C_T) and reflection coefficient (C_R) with structure and environment variables. The structure variable is the relative draft (s/h), and the environment variables are the relative depth (kh) and wave steepness (H_I/L).

Table 1 Structure variables

Structure Variables					
Variables	Symbol	Prototype		Model	
Draft of the skirt	s_1	3.00	m	25.00	cm
	s_2	2.00	m	16.70	cm
Chamber width	L_{c1}	4.60	m	55.00	cm

Table 2 Environment variables

Environment Variables					
Variables	Symbol	Prototype		Model	
Water depth	h	7.20	m	60.00	cm
Incident wave height	H_I	0.60–3.56	m	2.13–29.63	cm
Wave period	T	1.00–26.10	s	1.60–7.54	s

4. METHODS

4.1 Models

The SCSB configuration can be seen in Fig. 1 and 2, consisting of piles at the lower part and skirts with a chamber on the upper part. The skirt has no porosity attached to the upper part of the pile, and part of the skirt is submerged under the water level.

4.2 Laboratory Capacity and Wave Gauge Calibration

The capability of the wave generators to generate waves in terms of wave heights and periods is investigated by operating in various settings. The wave basin is 12.0 m long, 1.0 m deep, and 10.0 m wide. The wave basin can generate wave heights up to 30 cm and wave periods of up to 7 seconds.

Four-wave gauges are used and calibrated. The wave gauges are calibrated by comparing the wave heights measured visually at the wave basin with data recordings from the wave gauges. Table 3 shows the values of coefficient calibration.

Table 3 Values of coefficients of calibration (WG = wave gauge)

Water depth (h) [cm]	Coefficient of calibration			
	WG1	WG2	WG3	WG4
60	0.626	0.673	0.681	0.667

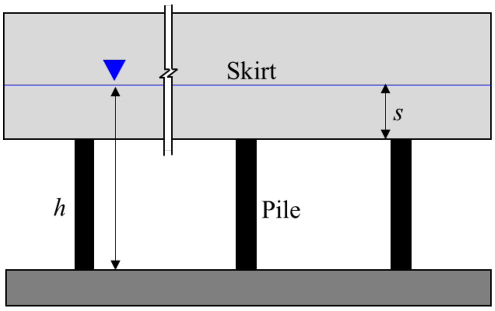

(a) Front view of SCSB

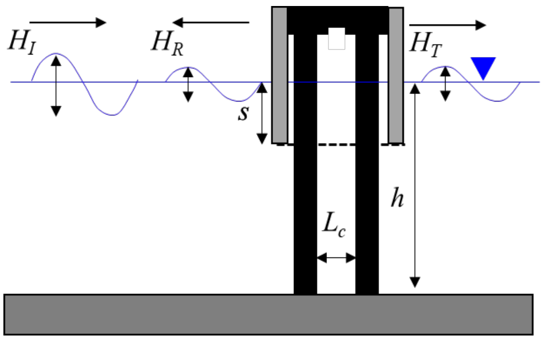

(b) Side view of SCSB

Fig. 1 Definition sketch of SCSB

h = water depth
s = draft of the skirt
H_I = incident wave height
H_T = transmitted wave height
H_R = reflected wave height
L_c = chamber width

4.3 Wave Basin Setup

The SCSB model, wave absorber, wave gauges, and wave maker are correctly installed in the wave basin, as seen in Fig. 3. The wave gauge position is arranged based on the Goda and Suzuki methods (1976) [10] and is formulated as in Eq. (5).

$$0.05 < \Delta\ell / L \quad (5)$$

$\Delta\ell$ = the distance between two wave gauges (m)
L = wavelength (m)

The closest wave gauge to the model should be placed at a distance of $0.2L$ from the model. From the equation, the distance between two wave gauges is 65 cm, and the model's distance from the wave gauges is 240 cm.

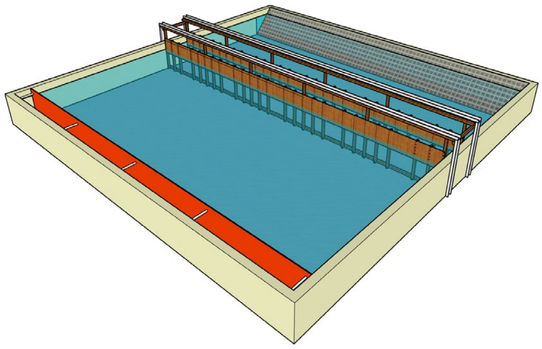

Fig. 2 Perspective view of SCSB in wave basin

5. EXPERIMENTS

The 54 scenarios of the experiments can be seen in Table 4. The scenario variables are the draft of the skirt, chamber width, water depth, the wave maker's motor speed, and waterboard reach length. The data are recorded for each scenario at 1-minute intervals. The incident wave height (H_I) and periods (T) are generated by the setup of the motor speed of the wave maker and adjusting the length of the waterboard reach.

6. DATA ANALYSIS

The incident wave data is recorded by wave gauges WG1, WG2, and WG3; WG4 records the transmitted wave data. The WG4 wave data is used to calculate the transmission coefficient (C_T), and the data from WG1, WG2, and WG3 are used to calculate the reflected coefficient (C_R)

The data recorded from the wave gauges are processed using zero-mean processes. First, the selection of time interval data to be analyzed is determined, i.e., the time-lapse in the wave record that has not been affected by the reflected waves. The result of the analysis is a non-dimensional graph of C_T and C_R versus the structure and environment variables.

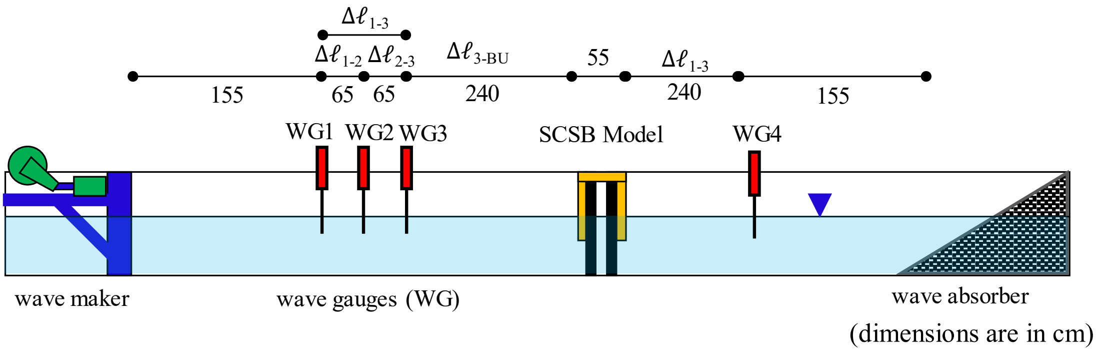

Fig. 3 Wave basin setup

Table 4 Scenarios of the experiment

Variables	Symbol	Model		Number of Scenarios
Draft of the skirt	s_1 s_2	25.00 16.70	cm cm	2
Chamber width	L_c	55.00	cm	1
Water depth	h	60.00	cm	1
The motor speed of the wave maker	*rpm*	200-1000	rpm	9
Length of waterboard reach	L_s	8.00 13.00 18.00	cm cm cm	3

6.1 Wave Transmission Analysis

The transmission coefficients (C_T) are the transmitted and incident wave heights ratio. The incident waves are calculated from the zero-up crossing data of the water level elevation, recorded by the wave gauges in front of the model.

The transmitted waves are the zero-up crossing of the water level elevation data from the wave gauges behind the model. The transmission coefficients (C_T) are defined in Eq. (6).

$$C_T = \frac{\overline{H_T}}{\overline{H_I}} \tag{6}$$

C_T = transmission coefficient
$\overline{H_I}$ = average incident wave height (m)
$\overline{H_T}$ = average transmitted wave height (m)

6.2 Wave Reflection Analysis

The wave reflection analysis is formulated using a method to resolve the incident and reflected waves from composite waves. The equation was first introduced by Goda and Suzuki [12]. Then, the reflection coefficient (C_R) analysis is calculated by comparing the incident wave energy and the reflection wave energy, as stated in Eq. (7).

$$C_R = \sqrt{\frac{E_R}{E_I}} \tag{7}$$

C_R = reflection coefficient
E_I = incident wave energy
E_R = reflected wave energy

The wave energy of the incident and reflected waves are calculated from Eqs. (8) and (9).

$$E_I = \int_{i=0}^{i=N} S_I(\omega)\, d\omega \tag{8}$$

$$E_R = \int_{i=0}^{i=N} S_R(\omega)\, d\omega \tag{9}$$

$S_I(\omega)$ = incident wave spectrum (m^2s)
$S_R(\omega)$ = reflected wave spectrum (m^2s)
ω = wave angular frequency (rad/s)

The incident and reflected wave spectra are calculated from the component of the amplitude spectrum according to Eqs. (10) and (11)

$$S_I(\omega) = \frac{\frac{1}{2} {a_{I_i}}^2}{\Delta\omega} \tag{10}$$

$$S_R(\omega) = \frac{\frac{1}{2} {a_{R_i}}^2}{\Delta\omega} \tag{11}$$

a_{I_i} and a_{R_i} are the amplitude of the spectrum components of the incident and reflected waves obtained from Goda and Suzuki (1976) [11]. The amplitude spectrum is calculated from Eq. (12) and Eq. (13).

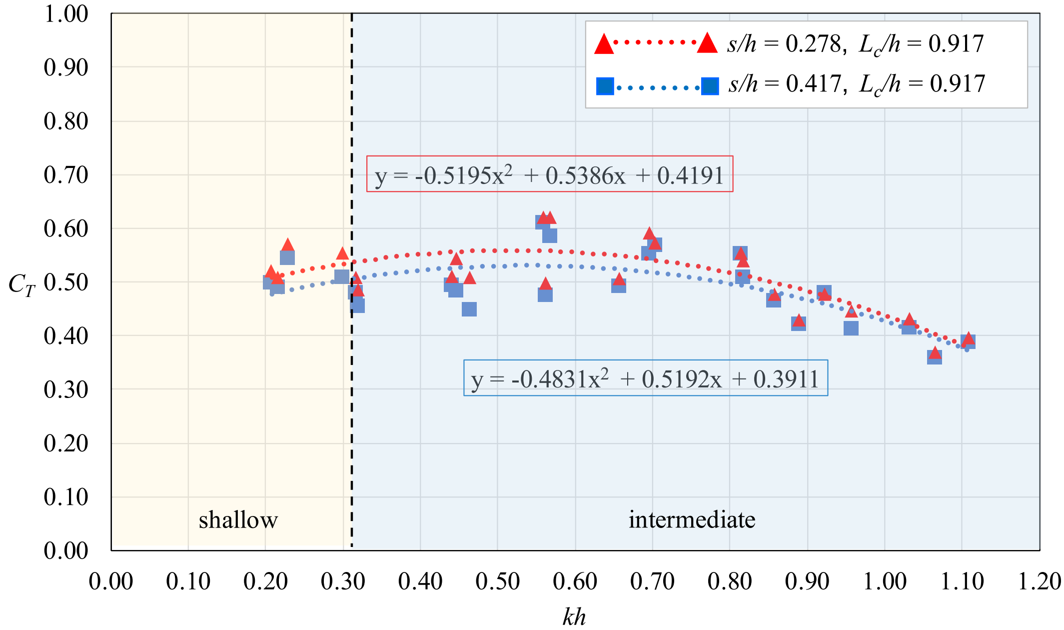

Fig. 4 Graph of transmission coefficent, C_T *vs* relative depth, *kh*

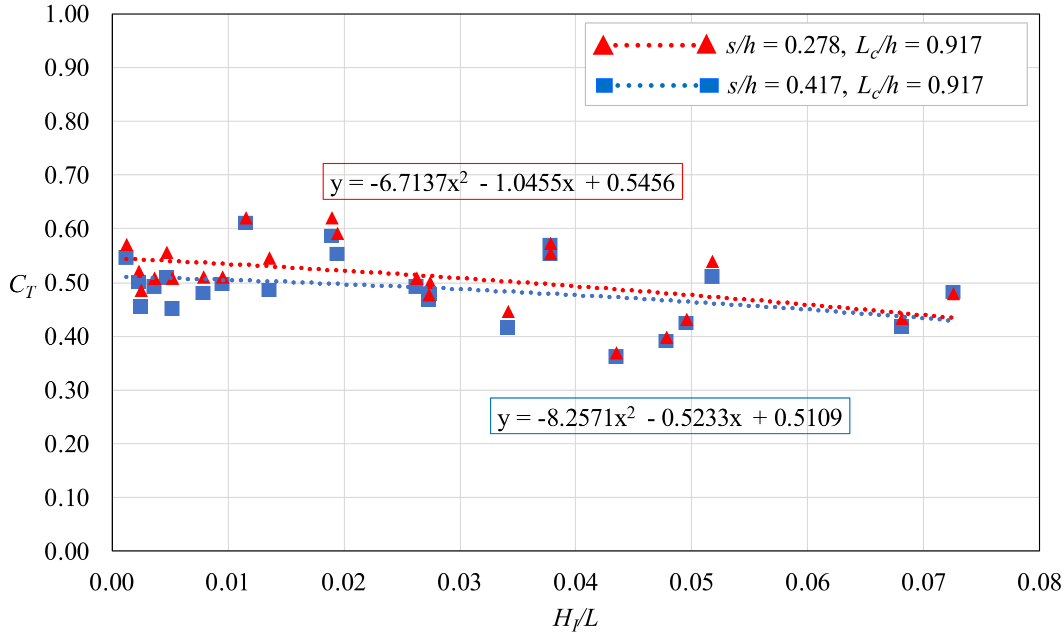

Fig. 5. Graph of transmission coefficent, C_T *vs* wave steepness, H_I/L

$$a_{I_i} = \frac{1}{2\left|\sin k_i \Delta\ell\right|}\left[\left(a_{2_i} - a_{1_i}\cos k_i\,\Delta\ell - b_{1_i}\sin k_i\Delta\ell\right)^2 + \left(b_{2_i} - b_{1_i}\cos k_i\Delta\ell + a_{1_i}\sin k_i\Delta\ell\right)^2\right]^{1/2} \quad (12)$$

$$a_{R_i} = \frac{1}{2\left|\sin k_i \Delta\ell\right|}\left[\left(a_{2_i} - a_{1_i}\cos k_i\,\Delta\ell + b_{1_i}\sin k_i\Delta\ell\right)^2 + \left(b_{2_i} - b_{1_i}\cos k_i\Delta\ell - a_{1_i}\sin k_i\Delta\ell\right)^2\right]^{1/2} \quad (13)$$

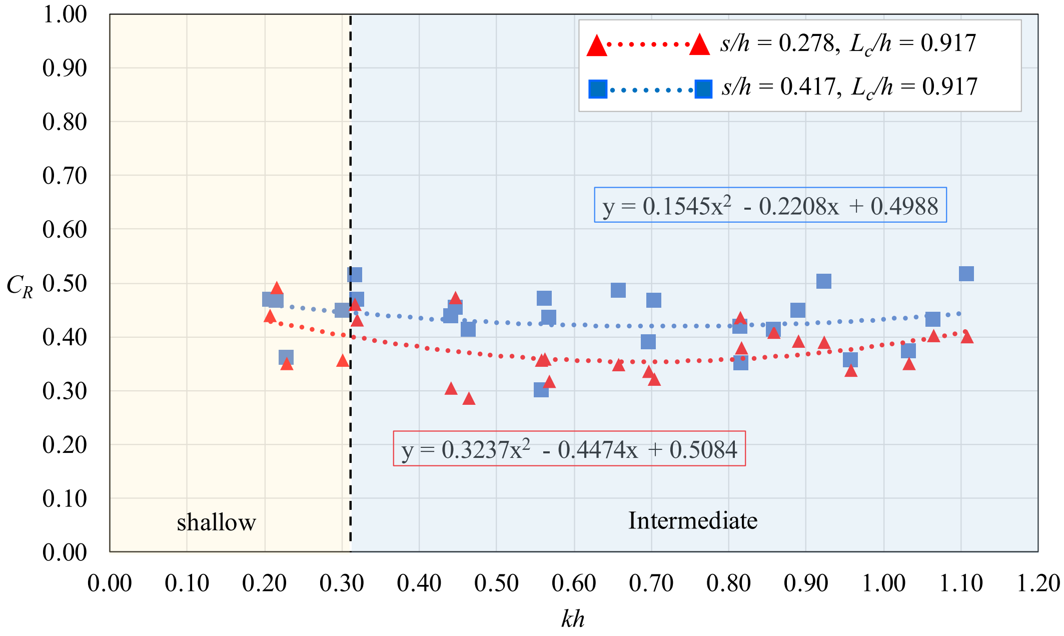

Fig. 6. Graph of reflection coefficient, C_R *vs* relative depth, *kh*

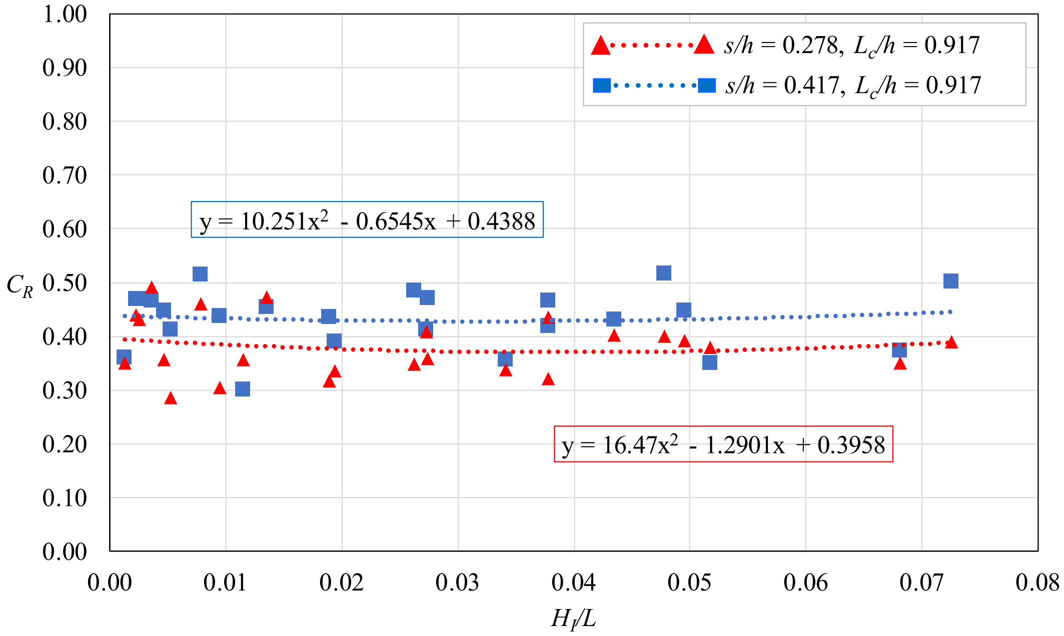

Fig. 7. Graph of reflection coefficent, C_R *vs* wave steepness, H_I/L

a_{1_i}, b_{1_i} = Fourier coefficient of WG1 data
a_{2_i}, b_{2_i} = Fourier coefficient of WG2 data
k = wave number (m^{-1})
L = wavelength (m)
$\Delta\ell$ = distance of WG1 and WG2 (m)

7. RESULTS AND DISCUSSION

The results of the three-dimensional physical model are explained by using non-dimensional plots in Figures 4–7. The plots show the relationship between the C_T and C_R values and the values of the environment variables, *kh* and H_I/L, as a function of structure variables, *s/h* and L_c/h, in the shallow and intermediate-depth water regions.

A comparison of the C_T and C_R values in the

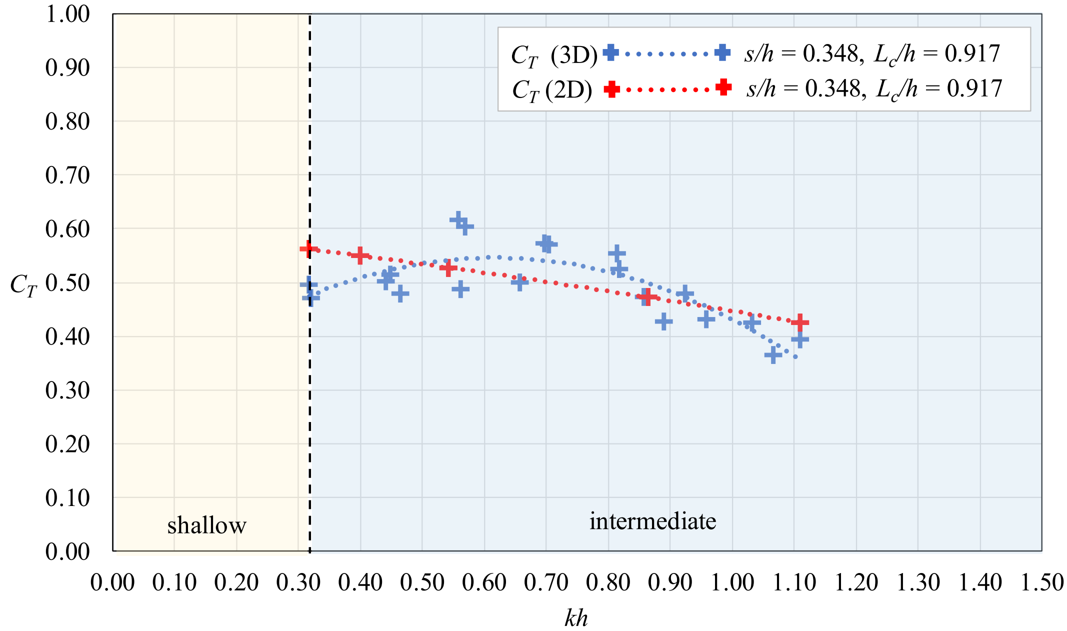

Fig. 8. Graph of transmission coefficient, C_T *vs* relative depth, *kh* SCSB 2D and 3D

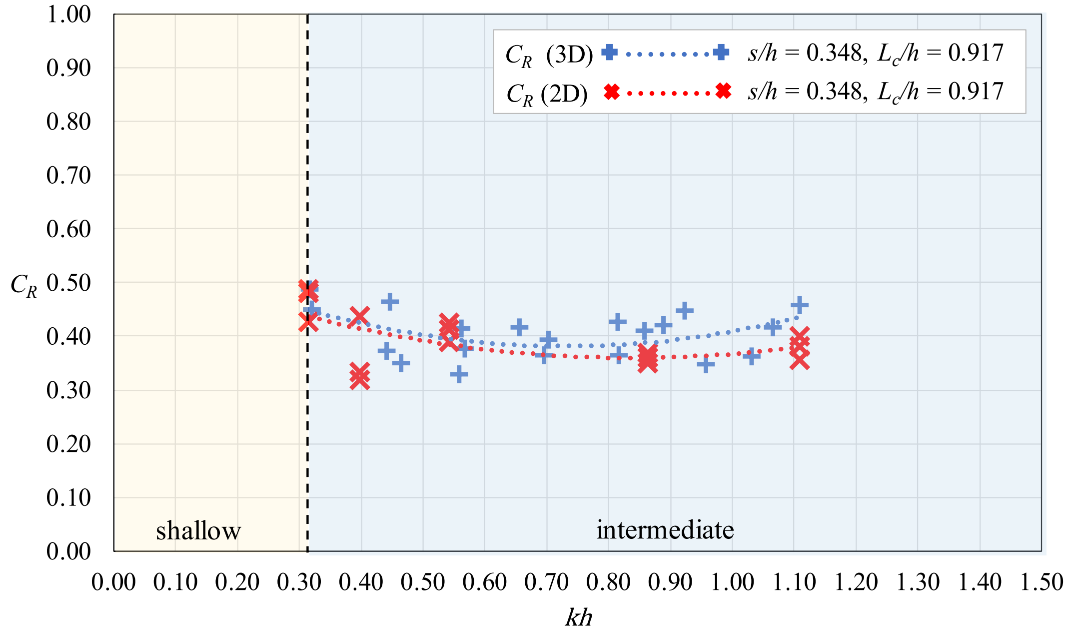

Fig. 9. Graph of reflection coefficient, C_R *vs* relative depth, *kh* SCSB 2D and 3D

same *kh* range of 2D and 3D models is presented in Figures 8 and 9.

7.1 Transmission Coefficient, C_T

Figure 4 shows the relation between C_T and *kh* as a function of *s/h* and L_c/h. As indicated by the figure, C_T decreases as *kh* increases, or the SCSB is more effective in intermediate-depth water ($0.36<C_T<0.62$) compared to shallow-depth water ($0.49<C_T<0.57$). From the relation of structure *s/h* and C_T, it is concluded that C_T increases as *s/h* decreases.

Figure 5 shows the relation between C_T and H_I/L as a function of *s/h* and L_c/h. As indicated by the figure, C_T decreases with the increase of H_I/L. Conversely, from the relation between *s/h* and C_T, it is concluded that C_T increases as *s/h* decreases.

7.2 Reflection Coefficient, C_R

Figure 6 shows the relation between C_R and *kh* as a function of *s/h* and L_c/h. The value of C_R in the intermediate water depth is 0.29< C_R <0.52. This is lower than those in the shallow water, which is 0.35<C_R<0.49, but the differences are insignificant. From the relation of *s/h* with C_R, it is concluded that C_R increases if s/h increases.

Figure 7 shows the relation between C_R and H_I/L as a function of *s/h* and L_c/h. The value of C_R does not change significantly to H_I/L. From the relation of *s/h* with C_R, it is concluded that C_R increases if *s/h* increases.

7.3 Comparison of C_T and C_R from SCSB 2D and 3D Physical Model

Figure 8 compares the C_T values in 2D and 3D dimensional physical modeling. The plot shows that the C_T value of the 3D physical model is lower than the 2D physical model by 0.007. Figure 9 compares C_R values from 2D and 3D physical modeling. The plot shows that the C_R value of the 3D physical model is higher than the 2D physical model by 0.009.

8. CONCLUSIONS

The average value of C_T in intermediate-depth water (0.32<*kh*<1.11) is 0.49 and in shallow water (0.21<*kh*<0.30), the average value of C_T is 0.53. It is concluded that SCSB is more effective in intermediate-depth water than in shallow water.

The average value of C_R in intermediate-depth water (0.32<*kh*<1.11) is 0.40, and in shallow water (0.21<*kh*<0.30), the average value of C_R is 0.42.

The results show that SCSB in shallow and intermediate-depth water is not significantly different.

The value of the relative draft (*s/h*) of the SCSB significantly influences the value of C_T and C_R. The increase in the *s/h* value (0.138) resulted in a decrease in the C_T value (0.023) and an increase in the C_R value (0.053). The C_T values of the 3D physical model are lower than the 2D and the C_R values of the 3D physical model are higher than the 2D.

9. REFERENCES

[1] Takahashi S., Breakwater Design (Tsinker G.P, Handbook of Port and Harbor Engineering), Chapman and Hall, USA, 1997, pp. 1-1054.

[2] Suh K.D., Shin S., Cox D.T., Hydrodynamic characteristics of curtain-wall-pile breakwaters, XXXI IAHR CONGRESS, Seoul, Korea, 2005, pp. 4002-4016.

[3] Koraim A.S., Hydrodynamic characteristics of slotted breakwaters under regular waves, Journal of Marine Science Technology, Vol. 16, 2011, pp. 331–342.

[4] Laju K., Sundar V., Sundaravadivelu R., Studies on pile supported skirt breakwater, The Journal of Ocean Technology, Vol. 2(1), 2007, pp. 1-22.

[5] Suh K.D., Jung H.Y., Pyun C.K., Wave reflection, and transmission by curtain wall pile breakwaters using circular piles, Ocean Engineering, Vol. 34, 2007, pp. 2100–2106.

[6] Wurjanto A., Ajiwibowo H., Zamzani R., 2D physical model to measure the effectiveness perforated skirt breakwater on the longwave category, Theory and Application of Civil Engineering Journal, Vol. 17, No. 3, 2010.

[7] Ajiwibowo H., Three-dimensional physical modeling on perforated skirt breakwater, International Journal of Engineering and Technology (IJET), Vol. 9, No. 6, 2017, pp. 4069–4080.

[8] Ajiwibowo H., 2-D physical modeling for measuring the effectiveness of single curtain pile foundation breakwater in intermediate water depth, International Journal of GEOMATE, Vol. 14, Issue 43, 2018, pp. 160–166.

[9] Ajiwibowo H., 2-D physical modeling to measure the effectiveness of perforated skirt breakwater for short period waves, ITB J. Eng. Sci, Vol. 43, No. 1, 2011, pp. 57–78.

[10] Wibowo A.A., Ajiwibowo H., Wurjanto A. Ghani A.Y., Two-dimensional physical modeling of Single Chamber Skirt Breakwater, International Journal of GEOMATE, Vol. 19, Issue 74, 2018, pp. 83–90.

[11] Hughes S.A., Physical Models and Laboratory Techniques in Coastal Engineering, World Scientific Publishing, Singapore, 1993, pp.1-568.

[12] Goda Y. and Suzuki T., Estimation of incident and reflected waves in random wave experiment, Coastal Engineering Proceedings, Vol. 1, No. 15, 1976, pp. 828-845.